Journal of the Optical Society of America B
OPTICAL PHYSICS

Comparison of Ag and Si nanoparticle arrays: mimicking subwavelength plasmonic field concentrations with dielectric components

E. Almpanis and N. Papanikolaou*

Institute of Nanoscience and Nanotechnology, NCSR "Demokritos," Patriarchou Gergoriou and Neapoleos Str. Ag. Paraskevi, GR-15310 Athens, Greece
**Corresponding author: n.papanikolaou@inn.demokritos.gr*

Received 4 November 2015; revised 24 November 2015; accepted 24 November 2015; posted 24 November 2015 (Doc. ID 253342); published 23 December 2015

We present a comparative theoretical study of the optical response of metallic Ag and dielectric Si sphere arrays on top of reflecting substrates. The interaction of particle modes with guided modes of the substrate leads to a rich optical spectrum. We design structures that sustain highly concentrated electromagnetic fields around periodic arrays of Si nanoparticles through the coupling of incident light to waveguide modes of a dielectric spacer. We discuss the origin of the different modes responsible for the reflectivity spectra of particle arrays and propose that all dielectric structures can support strong field enhancement which is similar to nanostructured metallic surfaces.

OCIS codes: (350.4238) Nanophotonics and photonic crystals; (240.6680) Surface plasmons; (290.4210) Multiple scattering.

http://dx.doi.org/10.1364/JOSAB.33.000099

1. INTRODUCTION

The emerging field of nanoplasmonics owes its reputation to the ability to confine and guide light down to the nanoscale, through the excitation of the so-called surface plasmons. These are combined oscillations of metallic electrons with an electromagnetic (EM) field that appear close to metal–dielectric interfaces and lead to increased sensitivity of the plasmonic resonance frequency to small changes in the optical properties of the dielectric [1]. For these reasons, controlling plasmonic excitation in nanopatterned metallic surfaces has proven useful for the development of chemical and biological sensors [2] and light harvesting [3] and also as a way to control light propagation using metamaterials [4] or even to achieve negative refraction [5]. Applications range from laser beam manipulation [4] to high-resolution microscopy [6]. Unfortunately, in many applications, Joule heating loss, inherent in plasmonic excitations, is problematic. To overcome this, hybrid photonic–plasmonic devices have been proposed [7,8], including metal–dielectric waveguides with reduced absorption losses [9–12], as well as nonmetallic structures based on dielectric nanostructured surfaces [13,14]. Recently, it has been recognized that high-refractive-index dielectrics could replace metallic components in particular applications to avoid the problem of strong light absorption in metals. Dielectric particles support Mie resonances which for particles with dimensions of the order of few hundred nanometers occur at visible and near-infrared frequencies [15]. The quality factor of such resonances increases by increasing the refractive index of the dielectric material [16]. High-refractive-index dielectric particles, like Si, are also considered for the design of all dielectric metamaterials [17], demonstrating effects like optical magnetism [18–23]. Arrays of such particles show total dielectric reflectance [24,25] and field enhancement [26].

Extensive studies are also reported for particle arrays on a slab substrate, since the combination of particle resonances with slab modes or surface states offers many possibilities. Characteristic examples are metallic [27–30] or dielectric [31–33] particles on a metallic film, where the optical response is determined by the interaction between the particle resonances in the array and the delocalized surface plasmon of the film. In this concept, complex surfaces can be designed to be antireflective surfaces or even perfect absorbers [28,34–36]. Although the role of plasmonic excitations in obtaining total absorbing surfaces is crucial, the interaction of a dielectric particle array with a Bragg multilayer as a substrate could also form total absorption resonances [37].

Moreover, when the metal film is relatively thin and the dielectric below the metal has a marginally higher refractive index than the dielectric on the particle side then we would observe the effect of extraordinary transmission and plasmon-induced transparency [27,38]. Such structures are often called metasurfaces due to the fact that they drastically alter the

distribution, phase, and polarization of an incident EM field with nanometer-thick structures [4]. Similarly, guided mode resonance filters [39] use periodic arrays to couple incoming waves to guided modes on a slab, resulting in controlled narrow-band reflection or transmission resonances [40].

In this paper we will attempt a comparative study of the optical properties of dielectric and metallic nanoparticle arrays. We identify all-dielectric structures where localized electromagnetic fields appear. Apart from the plasmonic excitation, we show that guided mode resonances lead to strong field localization comparable to the plasmonic one and compare metallic with dielectric structures.

2. RESULTS AND DISCUSSION

The optical properties of periodic nanoparticle arrays are affected by the optical modes of the isolated particles themselves, as well as the hybridizations of particle modes with their neighbors in a periodic arrangement or with optical modes of the substrate. It is useful to discuss the different optical interactions in structures of increasing complexity. Generally, nanoparticles that generate near-field can be classified in two categories: dielectrics, which support Mie resonances localized mainly inside the particle, and metals, where plasmonic oscillations provide strong near-field enhancements close to the surface of the particle. The difference between metallic and dielectric nanoparticles for near-field excitation has been extensively discussed by Terakawa *et al.* [41]. In this work we compare the optical response of dielectric and metallic nanoparticle arrays of the same geometrical parameters on top of reflecting substrates. The optical transmission and reflection are simulated with full electrodynamic solvers. We use our implementation of the layer multiple scattering (LMS) method [42,43] and compare it with the finite element method implemented in the commercially available COMSOL Multiphysics package. In all cases considered, materials are described using realistic optical constants fitted to experimental data.

A. Comparison of Periodic Arrays of Ag and Si Spheres

We will consider arrays of Si and Ag nanoparticles of the same radius $r = 65$ nm in air. For the isolated Si and Ag spheres the optical scattering cross section is shown in Fig. 1(a). The metallic particle shows a rather broad resonance centered around 425 nm, due to a dipolar plasmonic excitation, while for Si spheres the spectra have two resonances, a dipolar electric resonance found close to 460 nm and a dipolar magnetic resonance centered around 550 nm. The character of each mode is confirmed also by the electric field profiles.

By arranging the spheres in a square lattice with a lattice constant $a = 400$ nm, the reflectance spectra for light incident normally are shown in Fig. 1(b). For Si arrays, the spectra follow closely the behavior of the scattering cross section of the isolated spheres. This is due to the weak interaction between neighboring particles and the strong field confinement of the Mie resonances inside Si. The Fano-type resonance seen for wavelengths close to the lattice constant (400 nm) is the diffraction signature of the periodic arrangement. Generally, by optimizing the geometry, strong light absorption can be achieved, and similar Si particles arrays have been proposed as a perfect dielectric metamaterial reflector [24].

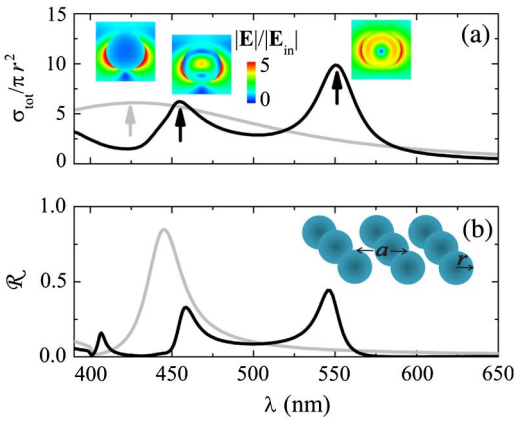

Fig. 1. (a) Sum of scattering and absorption cross sections normalized to the geometric cross section of Si (black line) and Ag (gray line) isolated spheres of the same radius $r = 65$ nm in air. The corresponding electric field profiles for light incident from the top, for a plane parallel to the polarization plane, cutting through the center of the spheres, for each mode at the frequencies indicated by the arrows, are also shown. (b) Reflectance spectra for normally incident light of Si (black line) and Ag (gray line) arrays of spheres ($r = 65$ nm) in a square lattice with a lattice constant of $a = 400$ nm in air.

The array of Ag spheres for the same geometry show a rather strong reflectance peak due to the dipolar plasmonic mode excitation for wavelengths around $\lambda = 450$ nm. This appears narrower compared to the peak of the total (including scattering and absorption) cross section of a single Ag sphere. The comparison of Si and Ag arrays, for this particular geometry, shows that the metallic structure is a stronger reflector close to 450 nm and also induces stronger electromagnetic fields near the metallic particles at the plasmon resonance. Moreover, the interaction between particle plasmons of the Ag particles leads to a stronger signature of the lattice for wavelengths close to the lattice constant.

The optical properties of metallic particle arrays can be tailored by optimizing the interaction of the array with carefully designed substrates [44–46], allowing symmetry to dictate the reflectivity spectra. In particular, the presence of a periodic array of particles on top of a dielectric slab can provide the extra momentum required so that optical slab modes are excited by a normally incident EM wave. Therefore, due to the rich spectra and strong field localization achieved, arrays of nanoparticles on top of a metallic film separated by a dielectric spacer is a popular system studied by several authors [27–30]. Most of the previous studies focus on the possibilities given by the plasmonic interaction to design functional surfaces that can be interrogated optically as a refractive index change sensor. We are interested in the possibility of metal-free surfaces that localize light in subwavelength volumes and seek to investigate relevant interaction mechanisms to achieve this.

We now compare Si and Ag sphere arrays on a 100 nm thick Ag film, separated with a SiO_2 spacer schematically shown in Fig. 2. Realistic optical constants, interpolated from tabulated

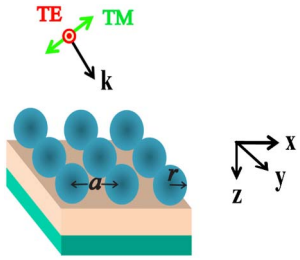

Fig. 2. Schematic of a nanosphere array on an Ag film, separated by a SiO_2 spacer.

data, are used for Si and Ag [47,48], while SiO_2 is described as a dielectric with a constant refractive index $n_{SiO2} = 1.46$. Generally, the different features in the spectra are due to particle modes (Mie or particle plasmon resonances), slab modes of the spacer, and surface plasmon resonances. For Si spheres, the optical reflectivity is shown in Fig. 3. The structure is opaque, and the excitation of the optical modes causes a series of absorption resonances. Our implementation of the LMS method is fast and accurate and the results are almost identical with the calculation of the finite element method (COMSOL), with the LMS method being roughly an order of magnitude faster. The strongest absorption is due to the excitation of the dipolar electric Mie modes close to 447 nm (i1) and the dipolar magnetic Mie modes around 540 nm (i4). These are very close to the positions of the modes for the arrays of Si spheres in air presented in Fig. 1 and show rather weak dispersion with the angle of incidence as shown in Figs. 3(b) and 3(c). For light incident normally, our structure gives a double resonance close to 475 nm which originates from a plasmon mode of the

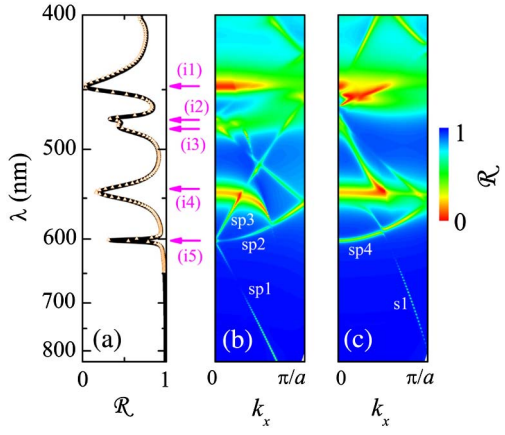

Fig. 3. (a) Reflectance spectra at normal incidence for a square array of Si spheres of radius $r = 65$ nm and lattice constant $a = 400$ nm, on top of a 100 nm thick Ag film, separated by a SiO_2 spacer of thickness 150 nm. Solid line, LMS calculations; symbols, COMSOL calculation. The labeled arrows indicate the positions of the different modes where reflectance reaches a local minimum. (b) Reflectance spectra for TM(p) polarized light incident with a parallel component of the wavevector k_x calculated with the LMS method. (c) Reflectance spectra for TE(s) polarized light incident with a parallel component of the wavevector k_x, calculated with the LMS method.

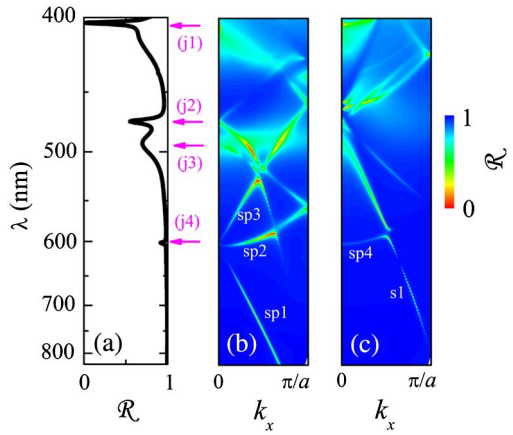

Fig. 4. (a) Reflectance spectra at normal incidence for a square array ($a = 400$ nm) of Ag spheres of $r = 65$ nm on top of 100 nm Ag film, separated by a 150 nm thick SiO_2 spacer. The labeled arrows indicate the positions of the different modes where reflectance reaches a local minimum. (b) Reflectance spectra for TM(p) polarized light incident with a parallel component of the wavevector k_x calculated with the LMS method. (c) Reflectance spectra for TE(s) polarized light incident with a parallel component of the wavevector k_x.

metallic substrate (shorter wavelength, i2) and a slab mode of the SiO_2 film (longer wavelength, i3) which is also seen in the dispersion diagrams for TE polarization (mode s1). The sharp drop just above $\lambda = 600$ nm (i5) is due to the surface plasmon mode localized at the metal–dielectric interface which splits in many branches (sp1, sp2, sp3, sp4) corresponding to different diffraction orders of the square lattice. This is seen in both TM and TE polarizations [32].

Replacing Si with Ag results in the calculated reflectance presented in Fig. 4(a). The surface plasmon appears at wavelengths similar to the Si arrays, as is clearly seen from the angular dispersion Figs. 4(b) and 4(c). For normal incidence, however, it is poorly excited and we observe only a small reflectance drop just above 600 nm (j4). The Ag structure favors the excitation of the film surface plasmon at 474 nm (j2), while a broader resonance centered close to 490 nm (j3), which is a hybrid mode with strong SiO_2 slab character, appears in the spectra. The stronger reflectance drop in this system occurs just above 400 nm and it is due to the diffraction of the lattice. These so-called Rayleigh–Wood anomalies have been studied previously toward a way to achieve strong light localization [49–53].

In Si arrays, the single-particle resonances are obviously different compared to Ag, but also the interaction strength of the different modes varies. The plasmon–plasmon interaction between the metallic particles is stronger than the interaction between Mie resonances in Si spheres, which results in a strong excitation of the Rayleigh–Wood modes in Ag arrays (mode j1). In contrast, in the geometry considered, Si spheres allow more efficient excitation of the film plasmons (compare mode i5 in Fig. 3 with mode j4 in Fig. 4) even for relatively thick spacers as we consider here. The field profiles of the structures with Si and Ag spheres are shown in Fig. 5. Important here is that the field is concentrated just outside the metallic particle but is mainly

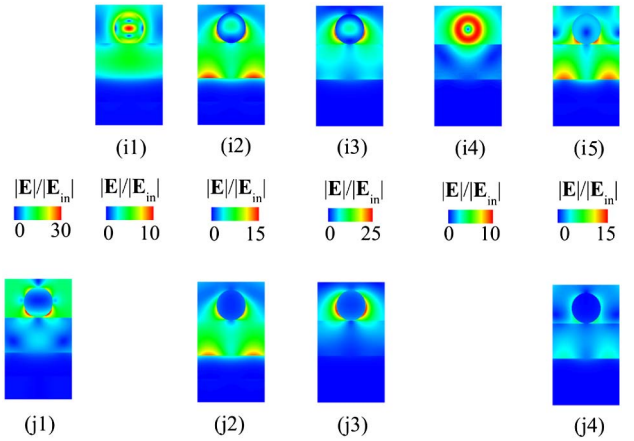

Fig. 5. Comparison of the field profiles for Si (upper plots) and Ag (lower plots) arrays for the different modes indicated by the arrows in Figs. 3 and 4 for a plane parallel to the polarization plane, cutting through the center of the spheres (x–z plane for a TM polarization as shown in Fig. 2).

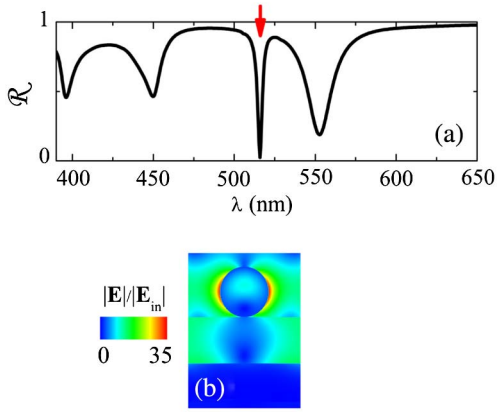

Fig. 6. (a) Reflectance spectra at normal incidence for a square array ($a = 480$ nm) of Si spheres ($r = 65$ nm) on top of a 100 nm thick Ag film, separated by a SiO_2 spacer of thickness 120 nm. (b) Field profile, for a plane parallel to the polarization plane, at the resonance indicated with the arrow in (a).

confined inside the Si particle. The resonances that originate from slab modes produce localized fields for both Si and Ag particles with hot spots in the region where the sphere touches the substrate. We also note that the field profiles of the Ag film surface plasmon modes excited by the Si sphere array are characterized by field enhancement in the vicinity, just outside of the dielectric spheres and not only close to the metallic film. Therefore, such modes can have high quality factors and will be sensitive to refractive index changes far away from the metallic parts of the structure and could be potentially useful in sensor applications.

The effect of the geometry on the different modes is an important issue. Changing the size of the spheres mainly affects the positions of the particle resonances, while variations of the spacer affect the spacer slab modes and the interaction of the particles with the surface plasmon at the metal–dielectric interface. The interaction of the different modes can be also modified by the lattice constant of the particle array.

In Fig. 6 we show the reflectivity for a surface with Si spheres ($r = 65$ nm), arranged on a square lattice of lattice constant $a = 480$ nm on top of Ag ($d_{Ag} = 100$ nm) with a SiO_2 spacer in between ($d_{SiO2} = 120$ nm). For these geometrical parameters the plasmon mode of the film is no longer discernible at normal incidence, while the SiO_2 slab mode, indicated by the arrow, is forming a total absorbing band, and the Mie resonances of the Si particles (compare Fig. 1) are clearly seen in the spectrum. The corresponding field profile, shown in Fig. 6(b), reveals that such modes can sustain highly localized fields outside the Si particles, and their wavelength strongly depends on the refractive index of the surrounding medium. In particular, for the air medium considered here ($n = 1$), the resonance indicated with an arrow in Fig. 6(a) shifts linearly to longer wavelengths with increasing n which results in a $S = \Delta\lambda/\Delta n = 210$ nm/RIU (RIU = refractive index units) and a figure of merit [54], FOM $= S/\text{FWHM} = 68$, which correlates with the resonance full width at half-maximum (FWHM). Such modes are tunable with the geometry, and at the same time relatively robust, since they do not depend on the exact particle shape or lattice type. Our results show that similar structures with a hexagonal lattice or arrays of cylinders are expected to have similar modes in their spectra with field localization, comparable to metallic nanoparticle structures. For the structure with a metallic substrate considered here (Fig. 6), this mode can be excited at small angles close to the normal since it is very close to the plasmon mode. On the other hand, the choice of a metal is not crucial and this particular mode will survive also for other metallic substrates.

B. Plasmon-like Field Concentration in Dielectric Structures

The metallic substrate can be replaced with a dielectric mirror. A Si sphere array with a 130 nm thick SiO_2 supporting spacer is placed on top of a five period Bragg multilayer of TiO_2(50 nm)/SiO_2(100 nm) with a period of $d = 150$ nm which has a gap for normally incident light, as is evident from the calculated reflectance shown with the dashed line in Fig. 7(b). The spheres are arranged in a square lattice ($a = 480$ nm), while the radii of the Si spheres are $r = 65$ nm [Fig. 7(a)]. This geometry supports various sharp resonant modes under normal incidence of light, as shown in Fig. 7(b), due to coupling into slab modes of the multilayer induced by the periodicity. Broader resonances are seen for wavelengths inside the bandgap of the Bragg mirror. The corresponding electric field profiles are shown in the inset. The mode at 505 nm (red arrow, left) can be compared to the mode shown in Fig. 6(b) and can sustain highly confined EM fields outside the nanoparticles and not only inside them like the Mie resonances. The mode seen at 560 nm (green arrow, right) is broader and is due to the magnetic Mie resonance of the Si spheres. These results demonstrate that highly concentrated electromagnetic fields can be achieved in dielectric nanoparticle arrays even in the absence of metallic components through the

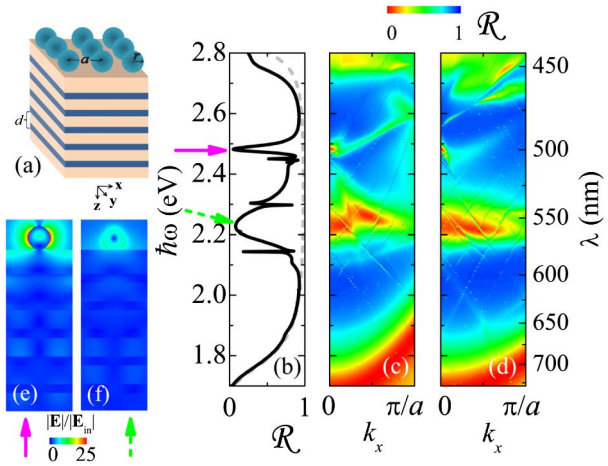

Fig. 7. (a) Schematic of a square array ($a = 480$ nm) of Si spheres ($r = 65$ nm) on top of a 130 nm thick SiO_2 layer on a Bragg multilayer of five TiO_2(50 nm)/SiO_2(100 nm) bilayers with $n_{TiO2} = 2.5$ (the thickness of each layer is given in parentheses). (b) The solid black line shows the reflectivity spectrum for normal incidence of light in the structure under consideration. The dashed gray line is the reflectivity of the Bragg multilayer stack without the sphere array. (c), (d) Reflectivity dispersion relations under off-normal incidence of light for TM(p) and TE(s) polarization, respectively. (e),(f) The electric field profile of the modes indicated with the red arrow (around 505 nm) and green arrow (around 560 nm), respectively. The cross section is for a plane parallel to the polarization plane.

coupling to guided modes of a dielectric spacer, while the presence of the reflector enhances the field.

3. CONCLUSIONS

We have compared the optical properties of Ag and Si periodic arrays on different substrates at visible and near-infrared wavelengths. Our results show many similarities between the metallic and dielectric systems. The strong coupling of incident light to waveguide modes of a dielectric slab through periodic arrays of high-refractive-index dielectric nanoparticles leads to a strong concentration of the electromagnetic field around the dielectric particles. Our analysis would be helpful in the design of metal-free environments that could enhance light emission or absorption with applications in light harvesting or refractive-index-based sensing.

REFERENCES

1. S. A. Maier and H. A. Atwater, "Plasmonics: localization and guiding of electromagnetic energy in metal/dielectric structures," J. Appl. Phys. **98**, 011101 (2005).
2. J. Homola, S. S. Yee, and G. Gauglitz, "Surface plasmon resonance sensors: review," Sens. Actuators B **54**, 3–15 (1999).
3. H. A. Atwater and A. Polman, "Plasmonics for improved photovoltaic devices," Nat. Mater. **9**, 205–213 (2010).
4. N. Yu and F. Capasso, "Flat optics with designer metasurfaces," Nat. Mater. **13**, 139–150 (2014).
5. C. Tserkezis, N. Papanikolaou, E. Almpanis, and N. Stefanou, "Tailoring plasmons with metallic nanorod arrays," Phys. Rev. B **80**, 125124 (2009).
6. A. Ono, J.-I. Kato, and S. Kawata, "Subwavelength optical imaging through a metallic nanorod array," Phys. Rev. Lett. **95**, 267407 (2005).
7. Y. Hong, M. Pourmand, and S. V. Boriskina, and B. M. Reinhard, "Enhanced light focusing in self-assembled optoplasmonic clusters with subwavelength dimensions," Adv. Mater. **25**, 115–119 (2013).
8. N. Kinsey, M. Ferrera, V. M. Shalaev, and A. Boltasseva, "Examining nanophotonics for integrated hybrid systems: a review of plasmonic interconnects and modulators using traditional and alternative materials," J. Opt. Soc. Am. B **32**, 121–142 (2015).
9. Y. Bian, Z. Zheng, X. Zhao, Y. Su, L. Liu, J. Liu, J. Zhu, and T. Zhou, "Guiding of long-range hybrid plasmon polariton in a coupled nanowire array at deep-subwavelength scale," IEEE Photon. Technol. Lett. **24**, 1279–1281 (2012).
10. Y. Bian and Q. Gong, "Metallic-nanowire-loaded silicon-on-insulator structures: a route to low-loss plasmon waveguiding on the nanoscale," Nanoscale **7**, 4415–4422 (2015).
11. Y. Bian and Q. Gong, "Deep-subwavelength light confinement and transport in hybrid dielectric loaded metal wedges," Laser Photon. Rev. **8**, 549–561 (2014).
12. R. F. Oulton, V. J. Sorger, D. A. Genov, D. F. P. Pile, and X. Zhang, "A hybrid plasmonic waveguide for subwavelength confinement and long-range propagation," Nat. Photonics **2**, 496–500 (2008).
13. S. Liu, M. B. Sinclair, T. S. Mahony, Y. C. Jun, S. Campione, J. Ginn, D. A. Bender, J. R. Wendt, J. F. Ihlefeld, P. G. Clem, J. B. Wright, and I. Brener, "Optical magnetic mirrors without metals," Optica **1**, 250–256 (2014).
14. J. C. Ginn, I. Brener, D. W. Peters, J. R. Wendt, J. O. Stevens, P. F. Hines, L. I. Basilio, L. K. Warne, J. F. Ihlefeld, P. G. Clem, and M. B. Sinclair, "Realizing optical magnetism from dielectric metamaterials," Phys. Rev. Lett. **108**, 097402 (2012).
15. P. Spinelli, M. A. Verschuuren, and A. Polman, "Broadband omnidirectional antireflection coating based on subwavelength surface Mie resonators," Nat. Commun. **3**, 692 (2012).
16. D. Kajfez and P. Guillon, *Dielectric Resonators* (Artech House, 1986), p. 547.
17. Q. Zhao, J. Zhou, F. Zhang, and D. Lippens, "Mie resonance-based dielectric metamaterials," Mater. Today **12**(12), 60–69 (2009).
18. A. Garcí-Etxarri, R. Gómez-Medina, L. S. Froufe-Pérez, C. López, L. Chantada, F. Scheffold, J. Aizpurua, M. Nieto-Vesperinas, and J. J. Sáenz, "Strong magnetic response of submicron silicon particles in the infrared," Opt. Express **19**, 4815–4826 (2011).
19. A. E. Miroshnichenko, W. Liu, D. Neshev, Y. S. Kivshar, A. I. Kuznetsov, Y. H. Fu, and B. Luk'yanchuk, "Magnetic light: optical magnetism of dielectric nanoparticles," Opt. Photon. News **23**(12), 35 (2012).
20. L. Shi, E. Xifre-Perez, F. J. Garcia de Abajo, and F. Mesegue, "Looking through the mirror: optical microcavity-mirror image photonic interaction," Opt. Express **20**, 11247–11255 (2012).
21. L. Shi, T. U. Tuzer, R. Fenollosa, and F. Meseguer, "A new dielectric metamaterial building block with a strong magnetic response in the sub-1.5-micrometer region: silicon colloid nanocavities," Adv. Mater. **24**, 5934–5938 (2012).
22. A. B. Evlyukhin, S. M. Novikov, U. Zywietz, R. L. Eriksen, C. Reinhardt, S. I. Bozhevolnyi, and B. N. Chichkov, "Demonstration of magnetic dipole resonances of dielectric nanospheres in the visible region," Nano Lett. **12**, 3749–3755 (2012).
23. P. Albella, M. A. Poyli, M. K. Schmidt, S. A. Maier, F. Moreno, J. J. Saenz, and J. Aizpurua, "Low-loss electric and magnetic field-enhanced spectroscopy with subwavelength silicon dimers," Phys. Chem. C **117**, 13573–13584 (2013).
24. B. Slovick, Z. Gang Yu, M. Berding, and S. Krishnamurthy, "Perfect dielectric-metamaterial reflector," Phys. Rev. B **88**, 165116 (2013).
25. A. B. Evlyukhin, C. Reinhardt, A. Seidel, B. S. Luk'yanchuk, and B. N. Chichkov, "Optical response features of Si-nanoparticle arrays," Phys. Rev. B **82**, 045404 (2010).
26. R. Sainidou, J. Renger, T. V. Teperik, M. U. González, R. Quidant, and F. J. García de Abajo, "Extraordinary enhancement all-dielectric light over large volumes," Nano Lett. **10**, 4450–4455 (2010).
27. N. Papanikolaou, "Optical properties of metallic nanoparticle arrays on a thin metallic film," Phys. Rev. B **75**, 235426 (2007).
28. N. Liu, M. Mesch, T. Weiss, M. Hentschel, and H. Giessen, "Infrared perfect absorber and its application as plasmonic sensor," Nano Lett. **10**, 2342–2348 (2010).

29. R. Ameling and H. Giessen, "Microcavity plasmonics: strong coupling of photonic cavities and plasmons," Laser Photon. Rev. **7**, 1–29 (2012).
30. C. Hägglund, G. Zeltzer, R. Ruiz, I. Thomann, H. B. R. Lee, M. L. Brongersma, and S. F. Bent, "Self-assembly based plasmonic arrays tuned by atomic layer deposition for extreme visible light absorption," Nano Lett. **13**, 3352–3357 (2013).
31. J. Grandidier, D. M. Callahan, J. N. Munday, and H. A. Atwater, "Light absorption enhancement in thin film solar cells using whispering gallery modes in dielectric nanospheres," Adv. Mater. **23**, 1272–1276 (2011).
32. M. López-García, J. F. Galisteo-López, C. López, and A. García-Martín, "Light confinement by two-dimensional arrays of dielectric spheres," Phys. Rev. B **85**, 235145 (2012).
33. Y. Yang, W. Wang, P. Moitra, I. I. Kravchenko, D. P. Briggs, and J. Valentine, "Dielectric meta-reflectarray for broadband linear polarization conversion and optical vortex generation," Nano Lett. **14**, 1394–1399 (2014).
34. C. Hägglund and S. P. Apell, "Resource efficient plasmon-based 2D-photovoltaics with reflective support," Opt. Express **18**, A343–A356 (2010).
35. M. Albooyeh and C. R. Simovski, "Huge local field enhancement in perfect plasmonic absorbers," Opt. Express **20**, 21888–21895 (2012).
36. M. B. Dühring and O. Sigmund, "Optimization of extraordinary optical absorption in plasmonic and dielectric structures," J. Opt. Soc. Am. B **30**, 1154–1160 (2013).
37. E. Almpanis and N. Papanikolaou, "Designing photonic structures of nanosphere arrays on reflectors for total absorption," J. Appl. Phys. **114**, 083106 (2013).
38. V. Yannopapas, E. Paspalakis, and N. V. Vitanov, "Electromagnetically induced transparency and slow light in an array of metallic nanoparticles," Phys. Rev. B **80**, 035104 (2009).
39. S. Tibuleac and R. Magnusson, "Reflection and transmission guided-mode resonance filters," J. Opt. Soc. Am. A **14**, 1617–1626 (1997).
40. P. Reader-Harris, A. Ricciardi, T. Krauss, and A. Di Falco, "Optical guided mode resonance filter on flexible substrate," Opt. Express **21**, 1002–1007 (2013).
41. M. Terakawa, S. Takeda, Y. Tanaka, G. Obara, T. Miyanishi, T. Sakai, T. Sumiyoshi, H. Sekita, M. Hasegawa, P. Viktorovitch, and M. Obara, "Enhanced localized near field and scattered far field for surface nanophotonics applications," Prog. Quantum Electron. **36**, 194–271 (2012).
42. N. Stefanou, V. Yannopapas, and A. Modinos, "Heterostructures of photonic crystals: frequency bands and transmission coefficients," Comput. Phys. Commun. **113**, 49–77 (1998).
43. N. Stefanou, V. Yannopapas, and A. Modinos, "MULTEM2: a new version of the program for transmission and band-structure calculations of photonic crystals," Comput. Phys. Commun. **132**, 189–196 (2000).
44. G. Gantzounis, N. Stefanou, and V. Yannopapas, "Optical properties of a periodic monolayer of metallic nanospheres on a dielectric waveguide," J. Phys. Condens. Matter **17**, 1791–1802 (2005).
45. S. Linden, J. Kuhl, and H. Giessen, "Controlling the interaction between light and gold nanoparticles: selective suppression of extinction," Phys. Rev. Lett. **86**, 4688–4691 (2001).
46. A. Christ, T. Zentgraf, J. Kuhl, S. G. Tikhodeev, N. A. Gippius, and H. Giessen, "Optical properties of planar metallic photonic crystal structures: experiment and theory," Phys. Rev. B **70**, 125113 (2004).
47. D. E. Aspnes, "Properties of silicon," in *EMIS Datareviews* (Inspec IEE, 1988).
48. B. Johnson and R. W. Christy, "Optical constants of the noble metals," Phys. Rev. B **6**, 4370–4379 (1972).
49. B. Auguié and W. Barnes, "Collective resonances in gold nanoparticle arrays," Phys. Rev. Lett. **101**, 143902 (2008).
50. V. G. Kravets, F. Schedin, and A. N. Grigorenko, "Extremely narrow plasmon resonances based on diffraction coupling of localized plasmons in arrays of metallic nanoparticles," Phys. Rev. Lett. **101**, 087403 (2008).
51. S. R. K. Rodriguez, A. Abass, B. Maes, O. T. A. Janssen, G. Vecchi, and J. Gómez Rivas, "Coupling bright and dark plasmonic lattice resonances," Phys. Rev. X **1**, 021019 (2011).
52. A. Tikhonov, N. Kornienko, J.-T. Zhang, L. Wang, and S. A. Asher, "Reflectivity enhanced two-dimensional dielectric particle array monolayer diffraction," J. Nanophoton. **6**, 063509 (2012).
53. E. Almpanis, N. Papanikolaou, B. Auguié, C. Tserkezis, and N. Stefanou, "Diffractive chains of plasmonic nanolenses: combining near-field focusing and collective enhancement mechanisms," Opt. Lett. **37**, 4624–4626 (2012).
54. X. Lu, L. Zhang, and T. Zhang, "Nanoslit-microcavity-based narrow band absorber for sensing applications," Opt. Express **23**, 20715–20720 (2015).